Information Sciences 476 (2019) 176–191

Contents lists available at ScienceDirect

Information Sciences

journal homepage: www.elsevier.com/locate/ins

# Component-based face recognition under transfer learning for forensic applications

Rupali Sandip Kute[a,*], Vibha Vyas[a], Alwin Anuse[b]

[a] Department of E&TC, Government College of Engineering Pune, Pune, Maharashtra, India
[b] Department of E&TC, Maharashtra Institute of Technology, Kothrud, Pune, Maharashtra, India

ARTICLE INFO

*Article history:*
Received 11 April 2018
Revised 11 October 2018
Accepted 12 October 2018
Available online 13 October 2018

*Keywords:*
Transfer learning
Component-based face recognition
Convolutional Neural Network
Partial face recognition

ABSTRACT

In numerous scenarios of forensic applications, only a partial face image is available for recognition purposes. Hence, the systems working on components of the face and partial face images have gained great importance. This paper proposes a novel approach for component-based face recognition and association under transfer learning and demonstrates that the knowledge gained from complete face images is transferred to classify components of the face. Three important components of a face, viz. ears, lips, and nose, are used for association and recognition. These components are unique, stable, and unaltered by the change in poses and expressions. Association is found between the face and nose, face and lips, as well as face and ears. Although, these face components and the face itself are from different domains, they share common information which is utilized to transfer the knowledge gained from one domain to another. Similarly, different types of half-faces are considered: left, right, upper, and lower half and left, right, upper, and lower diagonal for the association between complete and partial face images. Because of the association between a face and its different components, the proposed method can be applied to holistic face recognition, component-based face recognition and partial face recognition.



## 1. Introduction

Automatic face recognition methods aim to identify a particular person using full face images. The performance of these face recognition methods is affected by various aspects such as a change in pose, expressions, and illuminations. Component-based face recognition (CBFR) methods can be of significant help in overcoming these challenges. CBFR is recognition based on specific sub-regions of the face, viz. forehead, lips, chin, eyes, nose, mouth, ears, or eyebrows. The fundamental idea of the CBFR method is to compensate pose changes by preserving the shape and size of individual components of the face. Variations in illumination only affect a specific part of the face, hence, the CBFR system helps in improving accuracy. Global approaches that do not capture the minute differences of the components are captured by the CBFR method.

CBFR methods have a limited scope compared with automatic face recognition methods. Shedding inhibitions of facing a camera has resulted in an extremely large availability of full face images used for training and testing in face recognition methods. However, the CBFR method finds great potential in forensic applications where only a part or parts of the face may be available for recognition and it becomes very difficult to identify the suspect [39]. This challenge is an important

* Corresponding author.
*E-mail address:* rupali.kute@mitwpu.edu.in (R.S. Kute).

https://doi.org/10.1016/j.ins.2018.10.014
0020-0255/

motivation to investigate the CBFR method. In automatic face recognition methods, missing, incomplete, and noisy regions of the face reduce the recognition accuracy whereas in the CBFR system, investigators can select only particular part(s) of the face for identifying the suspect. Classifiers which are specially designed to recognize individual components of the face (nose, ears, and lips) achieve better accuracy compared with full face recognition classifiers. Components of the face, e.g., nose, lips, and ears, are unique, stable, and unaffected by make-up, poses, illuminations, and expressions [4,7,22].

This study proposes a novel approach for CBFR using a Convolutional Neural Network (CNN) architecture under a transfer subspace learning for forensic applications. Three important components of the face, viz. ears, lips, and nose, are considered individually for association and recognition. Additionally, half-face images (left, right, upper, and lower half, and left, right, upper, and lower diagonal) as well as full face images are considered for the purpose of association. Herein, a general framework for the association of face components or partial faces with a full face has been introduced. The framework comprises four stages. Stage I is a feature extraction phase in which the CNN is trained to extract features of different components. Stage II is a knowledge transfer phase in which the knowledge acquired from a full face sample is utilized while working with other components of the face. Stage III adopts an optimization function using the gradient descent method. Finally, stage IV is a classifier phase.

The novelty of the proposed approach is based on the following:

1. It is a CBFR method used for the association of an individual component with a full face;
2. All the holistic approaches assume that the probability distribution of training and testing samples are identical. CBFR under transfer learning minimizes the distribution difference between training and testing samples;
3. Ears are important components of a face, which is considered in the CBFR scheme. Existing partial face recognition methods have not considered the use of ears for the purpose of recognition;
4. A diagonal part of the face was not considered previously in the relevant literature for the purpose of recognition. In this paper, diagonal parts of the face are considered for the purpose of association and recognition; and
5. Because of the association among different face components and a full face, the proposed system works for both holistic and component-based recognition.

## 2. Related work

In the relevant literature, different CBFR methods use a variety of components and approaches for feature extraction and recognition. Buelthoff et al. [14] proved that the human visual system is inherently able to recognize faces based on the information extracted from isolated features (i.e., components). By comparing the optimal Bayesian integrator with the human component integrator, Gold et al. [33] proved that face processing is the result of integrating individual face component-based processing. In fact, any human being identifies a face by integrating individual facial features [12]. The comparison shows that the Bayesian framework works better than human prediction based on face components [33]. Furthermore, the approaches that use upper face components, viz. the forehead and eyes, exhibit a lower error rate and higher accuracy compared with approaches that use lower face components, viz. the mouth, chin, and nose [25].

For any face recognition technique, eyebrows are as important as eyes because they capture emotional expressions and non-verbal signals. Experimental studies by Jarudi et al. [40] demonstrated that the lack of processing of eyebrows from a face image leads to substantial performance degradation. Furthermore, results from physiological and neural studies show that face image processing is analyzed by configural information based on global facial features and component information based on local features such as the nose, eyes, and mouth [10,20]. Feature-based approaches combined with template matching techniques are successful in facial recognition. Typically, it is performed by matching three components of the face (mouth, nose, and left and right eyes) separately [13].

To improve the robustness against the change in poses, Principal Component Analysis (PCA) is applied on face components (eyes, nose, and mouth) in order to find the eigenspace [1]. Similarly, Linear Discriminant Analysis (LDA) is applied on five components of the face (left and right eye regions, left and right mouth regions, and the nose) using a single training sample [19] to determine the Fisher subspace. This method illustrated that CBFR is possible using a single training sample and can lead to better results compared with PCA. A combined method based on PCA and LDA is proposed by Cao et al. [15] for four face components to improve the performance of CBFR. In the elastic grid matching method [28], Gabor wavelets are used to extract the features of four face components at the grid point while recognition is performed using a wavelet coefficient. A probabilistic method using sub region matching is proposed by Martinez [46], to compensate for partly occluded, inaccurately localized facial features, as well as for facial expression variations; however, only a single training sample may be available for the system.

Bayesian framework and statistical learning theory are used to develop a model-free and non-parametric CBFR strategy [43]. Multiple descriptor methods are proposed [16] to overcome the problem of illumination and blurring. Composite sketches generated from face component are used to match with recent photos [31]. Gabor Filters and Zernike Moments are used as a feature descriptor to extract textural and shape features [34].

Some partial face recognition approaches need, as an input, only a part of the face such as eyes [2], nose [2,7], ears [2,4], left or right part of the face [35,49], or periocular region (viz. iris, retina, and sclera) [41]. Different descriptor methods are used to extract the features of the components, viz. the Scale Invariant Feature Transform (SIFT) descriptor [9,45] and the Multi-Keypoint Descriptor Sparse Representation-based Classification (MKD-SRC) [44]. These descriptor approaches do not

require any image pre-alignment. The Instance-to-class distance method is used to match a patch with the full face [38]. The Multiscale Double Supervision Convolutional Neural Network (MD-SCNN) [36] is proposed to extract the features of the eye region which improves accuracy. Three-dimensional partial face recognition using a single sample is proposed to address the problem of occlusions, missing parts, and data corruptions [29]. However, these methods are based on the assumption that the samples used for training and testing have the same probability distribution.

Based on the literature review, it should be noted that these methods are based on the assumption that the probability distribution of the training and testing samples is identical. Hence, the data used for testing degrades performance. CBFR is mainly focused on processing components such as eyes, nose, lips, and mouth and less attention is paid to an important component, i.e., ears. None of the partial face recognition methods considered a diagonal part of the face. More importantly, none of the methods emphasized the association between the face component and full face as well as the association between partial or half face and the full face of a person.

Hence, the proposed method is based on transfer learning that takes into account the probability distribution and different components of a face, viz. nose, lips, and ears, which are used for association with a full face. Furthermore, each part of the face (left, right, upper, and lower half, as well as left, right, upper, and lower diagonal) is considered individually for an association with a full face image.

## 3. CBFR under a transfer learning approach

Biometric studies have demonstrated the use of many prominent methods and algorithms for identifying a person based on his/her face biometrics. Parts of the face such as the nose, ears, and lips are proved to be unique biometrics. In their work, Evans and Moorhouse [47], proved that the nose is a unique biometric. Unlike other biometrics, the nose, lips, and ears are passive biometrics. The locations, shapes, directions, and structures of these biometrics are unique for human identification [5,21, 47]. The nose and ears biometrics are long-lasting, unlike face biometrics which change because of age, make-up, facial expressions, cosmetics, hairstyle, etc. The human face also changes because of expressions and emotions such as sadness, happiness, anger, and fear. The nose and ears biometrics do not change due to emotions, make-up, glasses, or facial hair [21, 47].

The advantage of the nose or ears biometric system is that their images can be acquired without any physical contact whereas in the case of fingerprint systems, physical contact is required to collect the images required for identification [21, 47]. Similarly, Choras [22] emphasized that lip features are unique and unalterable for every human being. Lip prints are used to support gender identification of a person. Human lip features may be processed for various scenarios such as speech recognition, multimodal audio-video speech recognition, speaker identification, and lip reading. The lip biometric is also a passive biometric [5]. That is the reason for selecting the nose, lips, and ears as crucial components in face recognition. The methods used for the recognition of a full face as well as face components, viz. nose, ears, and lips, are based on subspace learning techniques such as PCA [50], Fisher's LDA (FLDA) [27],and Locality Preserving Projections (LPP) [6], and are developed under the assumption that the training and testing samples are Independently Identically Distributed (i.i.d.). Pragmatically, a large amount of data should be used to train the system for accurate results. The difficulty involved in the classification is the unavailability of labeled data, as the data is too costly to be acquired and labeled. Hence, to facilitate the learning process, machine learning techniques can be deployed to use relevant and labeled data from various databases. Such databases assume that there is a similar distribution of training and testing data, i.e., that both share subspaces. This assumption is not true in the case of cross-domain applications. Hence, to improve accuracy, it is vital to transfer the knowledge gained in training to testing. This is feasible using transfer subspace learning.

Transfer learning is a technique which is used to overcome the limitation of learning with limited samples. To improve the learning process without being hampered b y a lot of labeled data, data from other databases can also be used. However, this creates misalignment between the source and the target data. Such an immediate utilization of source information can conceal the learning transfer, due to which, negative transfer occurs [48]. Transfer learning is a well-known learning method which considers helper (source) data. Knowledge can transfer from the source domain to the target domain for boosting learning execution [17]. Normally, the data is collected under varied conditions from diverse environments [32] due to which they can have different distributions. Hence, the system performs poorly for samples from different domains.

Transfer subspace learning is used in many applications such as kinship verification, where young parent's data is used as an intermediate distribution to bridge gaps among children and old parents [30]. The old parent's dataset is used to predict children's labels. Knowledge can be transferred between different domains like cross-database age estimation, cross-dataset facial expression, as well as sign language classification where the knowledge gained to classify one language, is used to classify another language [17,32]. In all these cases, the source and target domains are different. Transfer subspace learning is used in cross-domain discriminative Hessian Eigenmaps for a web image annotation [18]. Here, the quadratic distance between the distribution of the training samples and the testing samples is minimized.

Hou et al. [37] proposed an effective transfer learning framework to reduce time and space cost as well as to overcome the over-fitting problem. Enhanced subspace clustering methods handle abundant and complex data for optimizing the clustering results [24]. Transferred centroid regularization is proposed [23] to address multiple source domains and a single target domain. The cross-resolution problem where high-resolution face images should match with low-resolution images is successfully resolved using transfer learning [11]. In medical applications too, where data is collected from different scanners or imaging protocols, performance improves when using transfer learning [26].


**Fig. 1.** CBFR block diagram of the biometric association.

Deep transfer learning is used to overcome the problem of insufficient training data. The association of two different biometric faces and fingerprints is possible using transfer subspace learning [42]. A novel deep transfer learning for face recognition task has been proposed by Anuse and Vyas [3].

The approach proposed in this study explores a discriminative subspace in the source domain for utilizing it in the target domain. The difference between the distributions amongst these domains is eliminated and the maximum discriminative information is transferred. In transfer learning, when the samples were unlabeled, different types of source information were utilized, viz. feature sharing from the auxiliary domain [30,32], data from various feature spaces, and samples from auxiliary tasks. The model and the way of utilizing the auxiliary information varied depending on the application.

The present work utilizes Bregman divergence-based regularization which can be applied to the contemporary dimensionality reduction algorithm, FLDA. Hence, by combining this with regularization, a subspace can be acquired where the distinction between training and testing biometrics is limited. As a result of this, the i.i.d. assumption is shown to be valid in the learning subspace [32]. Since it protects specific data, information from different classes can precisely be isolated.

This paper proposes that using the combination of subspace learning and regularization, one can integrate the face and components of the face, i.e., the nose, lips, and ears, or the half-face. For deploying forensic applications, this model can be used for integrating features in order to identify a suspect. This paper considers the associations between the face and nose, the face and lips, and the face and ears. They are all from completely different domains but the face and its components share common information. This brings biometrics together in a common subspace by minimizing the probability distribution between them. FLDA is used as an objective function for feature selection and subsequent integration with transfer subspace learning. The proposed model is then tested and verified using a KNN classifier.

## 4. Proposed framework

The block diagram for the proposed CBFR under transfer learning is shown in Fig. 1. The first task in the process is to resize the original image to $32 \times 32 \times 3$ pixels, and then extract features using CNN as a deep learning network. Extracted features are given to the combined transfer FLDA and regularization block for dimensionality reduction and minimization of the probability distribution difference between different domains. Finally, the K-nearest neighbor classifier is used for classification.

### *4.1. Transfer subspace learning framework*

A subspace learning algorithm is used to solve the problem of classification using an objective function. For the task of classification, consider $m$ training samples with $I$as an input and $t$ as a target,$S = \{(I_1, t_1), (I_2, t_2), (I_3, t_3), \ldots I_m, t_m)\}$, and $n$ number of testing samples $T = \{(I_{m+1}), (I_{m+2,}), (I_{m+3}), \ldots (I_{m+n})\}$. These samples are drawn from high-dimensional subspace$R^D$. The subspace learning algorithm finds a low-dimensional subspace $R^d$. A linear function$y = M^T I$, where $M \in R^{DXd}$ and $y \in R^d$ will find a low-dimensional space $R^d$. The objective function can be specified as

$$M = \arg\min F(M) \tag{1}$$

subject to constraint $M^T M = I$. The objective function $F(M)$ is used to reduce the classification error. Eq. (1) works well if the samples drawn from the training and testing domains are i.i.d. However, in practice, the distribution of training samples $P_S$ and the distribution of testing samples $P_T$may be different. In such cases, the learning framework given in Eq. (1) fails. To overcome this problem, Bregman divergence-based regularization $D_M(P_S||P_T)$ which measures the distribution difference between training and testing samples in the projected subspace $M$ is used [32]. Therefore, a new framework adapted for transfer subspace learning by modifying Eq. (1) is given as Eq. (2) below:

$$M = \text{argmin}\{F(M) + \lambda D_M(P_S \,||\, P_T)\} \tag{2}$$

with the constraint $M^T M = I$. In Eq. (2), $\lambda$ is the regularization parameter which controls the trade-off between $F(M)$ and $D_M(P_S||P_T)$. The solution of Eq. (2) is obtained using a gradient descent algorithm given as

$$M_{k+1} = M_k - \eta\left(\frac{\partial F(M)}{\partial M}\right) + O \tag{3}$$

where $O = \frac{\partial D_M(P_S \,||\, P_T)}{\partial M}$ and $\eta$ is the learning rate.

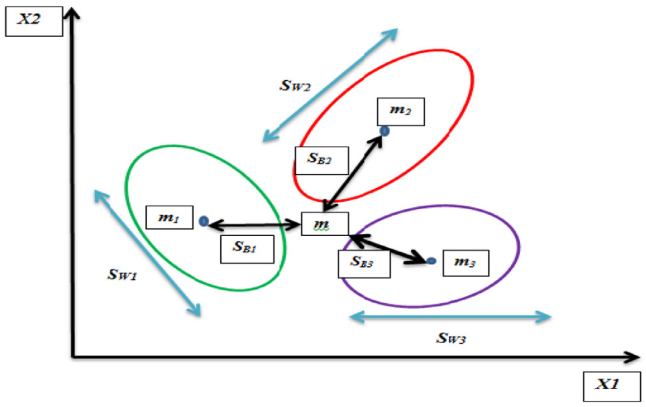


**Fig. 2.** The separation between 'within-class scatter' and 'between-class scatter'.

### 4.2. FLDA

The objective of FLDA is to achieve dimensionality reduction while conserving maximum class discriminative information. It is a supervised method which considers label information of samples. The purpose of FLDA is to maximize the separation between different classes. It creates a new axis to distinguish the data. For the two-class problem, FLDA finds a projection line and for the multiclass problem, it finds the subspace. It preserves a class structure in lower dimensional space and reduces high dimensional face features to low dimensional features by maximizing the ratio of the 'between-class scatter' to that of the 'within-class scatter' matrix.

As shown in Fig. 2, for the multi-class problem, 'between-class scatter' and 'within-class scatter' should be maximum and minimum respectively to achieve a precise separation between different classes. Consider a set $I = \{I_1, I_2, I_3, \ldots I_k\}$ describing the feature vector of $k$ face images, where $I_i$ is a vector of $n$ features. All samples of set $I$ belong to one of the classes mentioned in set $C = \{C_1,\ C_2,\ C_3 \ldots C_l\}$. For $C$number of classes, FLDA gives $(C-1)$number of projections $Y = \{y_1, y_2,\ y_3, \ldots y_{c-1},\}$ and the same number of projection vectors $M_i$is arranged in a matrix.

$M = [M_1|M_2|M_3| \ldots M_{C-1}]$ where the objective is to obtain a linear function $y = M^T I$

Steps to determine objective function $F(M)$ are the following:

(1) Consider $I$as an input feature vector;
(2) Calculate the 'within-class scatter' matrix $S_w$

$$S_W = \sum_{i=1}^{C} S_i \tag{4}$$

where

$$S_i = \sum_{i \epsilon C_i} (I_i - m_i)(I_i - m_i)^T \tag{5}$$

and

$$m_i = \frac{1}{N_i} \sum_{i \epsilon C_i} I_i \tag{6}$$

Here, $m_i$ is the mean, $S_i$ is the scatter and $N_i$are the numbers of samples belonging to class$C_i$.

(3) Calculate the 'between-class scatter' matrix $S_B$

$$S_B = \sum_{i=1}^{C} n_i (m_i - m)(m_i - m)^T \tag{7}$$

Here, $C$ is the total number of classes, $n_i$ is the total number of feature vectors that belong to the class $i$, $m_i$ is the mean of class $i$ and $m$ is the overall mean.

(4) Calculate ${S_W}^{-1} S_B$.
(5) Evaluate eigenvectors corresponding to eigenvalues of${S_W}^{-1} S_B$.
(6) $V$number of eigenvectors are selected depending upon the highest number of eigenvalues.
(7) Selected highest eigenvalues$V$will give the vector $M$.

Hence, the objective is to minimize $S_W$ and maximize $S_B$, therefore

$$F(M) = tr^{-1}\left(M^T S_B M\right) tr\left(M^T S_W M\right) \tag{8}$$

The derivative of $F(M)$ with respect to $M$ is taken to achieve minima which given in Eq. (9):

$$\frac{\partial F(M)}{\partial M} = 2tr^{-1}\left(M^T S_B M\right) S_W M - 2tr^{-2}\left(M^T S_B M\right) tr\left(M^T S_W M\right) S_B M \tag{9}$$

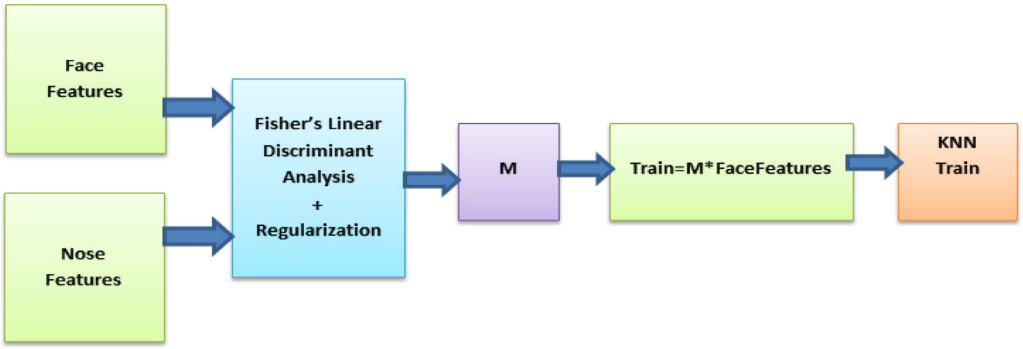


**Fig. 3.** Training phase.

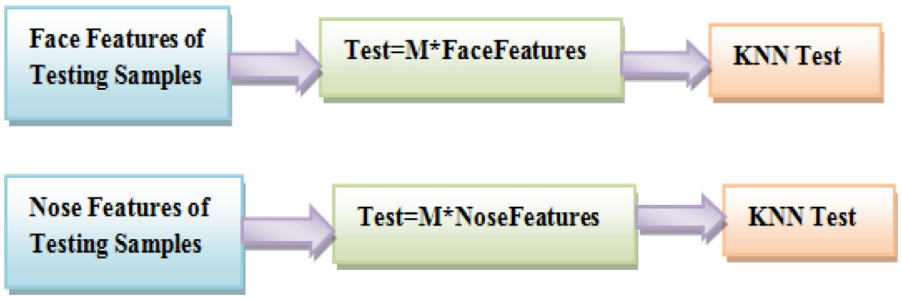


**Fig. 4.** Testing phase.

The limitation of FLDA is that it requires the samples used for training and testing to follow the same Gaussian distribution. It neglects prior information of the probability distribution. Therefore, for this ill-posed problem, it is necessary to consider regularization for diminishing the difference between probability distributions. Si et al. in [32] proposed a Bregman divergence-based regularization method to measure the difference between two probability distributions. FLDA is used for discrimination among different classes and, at the same time, regularization minimizes the distance between probability distributions.

The aim of the association between a face and its components is to extract their features for creating a common subspace. For example, to associate a face with the nose, full face features are extracted using CNN and are projected on a reduced subspace using FLDA. With the same projection matrix, nose features are also projected onto the reduced subspace. Thus, facial and nasal features of the same person share the same class.

Bregman divergence minimizes the difference between probability distributions of training samples $P_S$ and testing samples $P_T$ and brings them together to a common subspace. $P_S$ represents the probability distribution of facial features and $P_T$ represents the probability distribution of nasal features. Therefore, FLDA discriminates between classes and Bregman divergence brings them together. A detailed training procedure is shown in Fig. 3. Features of the face and its components e.g. nose are extracted using CNN. After applying FLDA to the face feature vector, it gives a reduced dimension space which is used to reduce the dimension of both biometrics. Projected subspaces of the face and nose biometrics along with Bregman divergence are used for minimizing the distribution. Finally, a new subspace $M$is achieved as given in Eq. (3). As shown in Fig. 4, a new subspace $M$ is used in the testing phase to classify the samples as either a full face or a part of the face.

### 4.3. CNN

CNN belongs to the class of deep networks used in machine learning. Here, the feed forward artificial neural network is used to visualize image data like the human visual cortex. CNN is an unsupervised semi-parametric method to extract features as well as work as a classifier. It extracts the features independently without any prior knowledge of the image. CNN is used for feature extraction of face and nose images. It comprises the input layer, convolution layer, pooling layer, and fully connected layer. The convolution layer consists of a bank of filters and it performs the convolution operation on the input image.

Layer I1 is an input layer, the input is a $32 \times 32 \times 3$ colour image.

Layer C2 is a convolution layer with 20 filters with $5 \times 5$ kernels and stride 1 with zero padding. Therefore, the total number of trainable parameters or weights is $5 \times 5 \times 3 \times 20 = 1500$. The output of this layer is a $28 \times 28 \times 20$ feature map.

Layer R3 is a rectified linear unit layer. After a convolution layer, the R3 layer applies an additive bias and sigmoid nonlinearity to each feature map.

Layer P4 is a pooling layer. The output of the $28 \times 28 \times 20$ feature map is given as an input to the pooling layer. Each map is then sub-sampled using a max pooling layer on $2 \times 2$ windows. It gives a feature map with a $14 \times 4 \times 20$ size. Layer P4 has no trainable weights.

Layer C5 is a convolution layer with 16 filters with $5 \times 5$ kernels and stride 1 with zero padding. Therefore, the total number of trainable parameters or weights is $5 \times 5 \times 20 \times 16 = 8000$. The output of this layer is a $10 \times 10 \times 16$ feature map.

Layer R6 is a rectified linear unit layer. After the convolution layer, the R6 layer applies an additive bias and sigmoid nonlinearity to each feature map.

Layer P7 is a pooling layer. The output of the $10 \times 10 \times 16$ feature map is given as an input to the pooling layer. Each map is then sub sampled using a max pooling layer on $2 \times 2$ windows. It gives a feature map of the size of $5 \times 5 \times 16$. Layer P7 has no trainable weights.

Layer F8 is a fully connected layer. The number of neurons in the fully connected layer depends upon the number of classes. In the proposed approach, for 100 classes the total number of feature maps is 100 and the number of trainable parameters or weights is $5 \times 5 \times 16 \times 100 = 1024$.

Layer S9 is a softmax layer and features are extracted from the same layer. Due to the presence of 100 neurons in the last layer, the number of features for every image is 100.

## 5. Dataset

For the purpose of experimentation, the Computer Vision Research Projects Faces94 standard face database was selected. It contains face images of 153 individuals with 20 images per person. To the best knowledge of the authors, there is unavailability of publically available face database which contain separate components of the face, viz. nose, lips, and ears, half faces [(left, right, upper, lower) half, (left, right, upper, lower) diagonal] of the same person. Therefore, datasets are prepared by cropping different parts of a face from the Faces94 standard database. One hundred individual face images having all components articulately visible were chosen randomly from the standard database. From this, a subset of four datasets of noses, left and right ears, and lips components and eight datasets of half faces (left, right, upper, and lower half, as well as left, right, upper, and lower diagonal) were prepared.

Based on the four datasets for the components, viz. nose, ears (left and right), and lips, eight experimental sets were built, as given below:

(1) F + N2F: a combination of a full face (F) and a nose component (N) is applied for training and a full face is used for testing.
(2) F + N2N: a combination of a full face (F) and a nose component (N) is applied for training and a nose component is used for testing.
(3) F + L2F: a combination of a full face (F) and a lip component (L) is applied for training and a full face is used for testing.
(4) F + L2L: a combination of a full face (F) and a lip component (L) is applied for training and a lip component is used for testing.
(5) F + LE2F: a combination of a full face (F) and the left ear component (LE) is applied for training and a full face is used for testing.
(6) F + LE2LE: a combination of a full face (F) and the left ear component (LE) is applied for training and the left ear is used for testing.
(7) F + RE2F: a combination of a full face (F) and the right ear component (RE) is applied for training and a full face is used for testing.
(8) F + RE2RE: a combination of a full face (F) and the right ear component (RE) is applied for training and the right ear is used for testing.

Sample images of the face, lips, ears (left and right), and nose biometrics are shown in Figs. 5 and 6. Furthermore, sample images of half faces (left, right, upper, and lower half, as well as left, right, upper, and lower diagonal) are shown in Figs. 7–10.

## 6. Experimentation and result analysis

### *6.1. Full face vs. face component recognition*

As CNN is used for feature extraction, an important aspect is the number of images used for training. Two types of experiments were performed on the above mentioned eight datasets: (1) the number of full face images used for training the CNN architecture varies from 10 images of each person to 1 image of each person, i.e., 10 images of each person (1000 images of each component) was used for training and 10 images of each person per component (1000 images) were used for testing; (2) the number of full face images used for training the CNN architecture is kept constant, 10 images per person and the number of images per person per component varies from 10 images per person to 1image per person for training and 10 images per person (1000 images per component) were used for testing. Fig. 11 depicts the component recognition rates versus the number of the full face images used for training the CNN architecture under F + N2N, F + L2L, F + LE2LE,

(a) (b)

**Fig. 5.** Sample images of (a) face biometric Faces94 and (b) cropped images of face component lip.

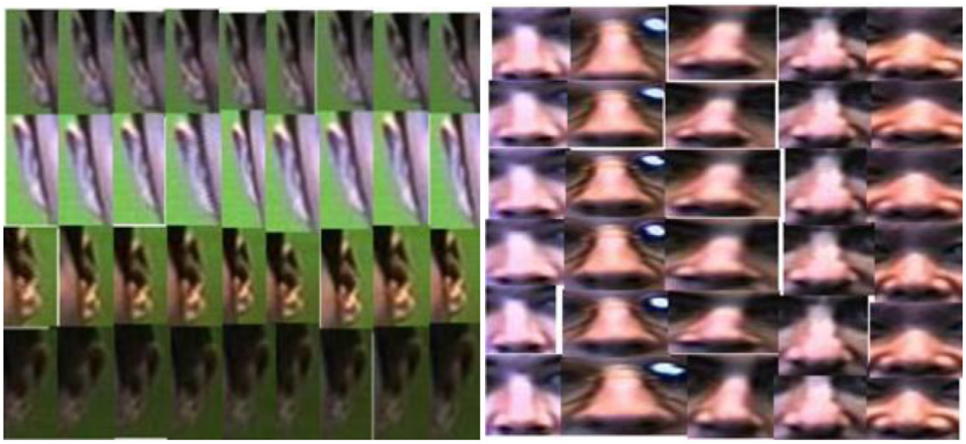

(a) (b)

**Fig. 6.** Sample images of (a) cropped images of the left and right ears and (b) cropped images of noses.

F + RE2RE experimental settings. It is observed that usage of a nose component achieved maximum accuracy compared with other components. The right ear component accuracy is nearly 75% which is less compared with other components because the images of the right ear are not clearly visible in the referred database. As the number of full face images used for training decreased, the recognition rate also decreased.

Fig. 12 represents the face recognition rates versus the number of images per person per component used for training the CNN architecture under F + N2N, F + L2L, F + LE2LE, F + RE2RE experimental settings. It is observed that for the full face, a recognition rate of 98% has been achieved even if combined with any component. As the number of images used for training decreased, the recognition rate slightly diminished.

Fig. 13 illustrates the convergence of objective function. It exhibits the property of a gradient descent algorithm: as the number of iterations increases, the objective function converges. This trend is observed in all the different experimental settings. However, only the analysis of deep transfer FLDA on F + L2F and F + L2L experimental settings is shown in Fig. 13. It represents the trends of deep transfer FLDA's objective function value and its recognition rate versus the number of iterations. It demonstrates that the objective function decreases as the number of iterations increases. Therefore, it proves that this algorithm can determine the optimum solution for the problem of associating different components and full face images. The initial value of the objective function is taken from the subspace obtained by FLDA.

Table 1 provides the comparison performed at feature extraction level using a Histogram of a gradient (HOG), Gabor features by creating a Gabor filter bank of size $5 \times 5$ and CNN. It depicts that CNN feature extraction outperforms handcrafted features.

A confusion matrix is a table used to describe the performance of the classifier on the set of test data for which the labels are known. The outcome of the confusion matrix is of true positive, true negative, false positive, and false negative values. Using these values, various important statistical measures are derived such as the error-rate, accuracy, specificity, sensitivity, precision, and ROC (Receiver Operating Characteristics). To analyze the performance of the classifier, two experiments were

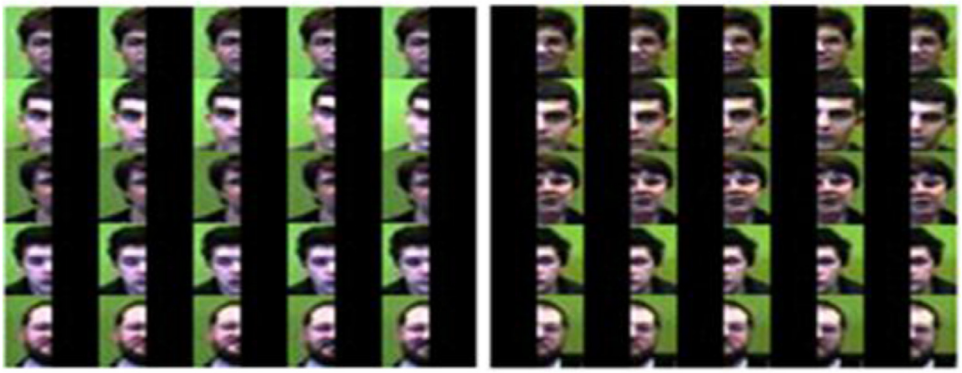


**Fig. 7.** Sample images of (a) the left half-face and (b) the right half-face.

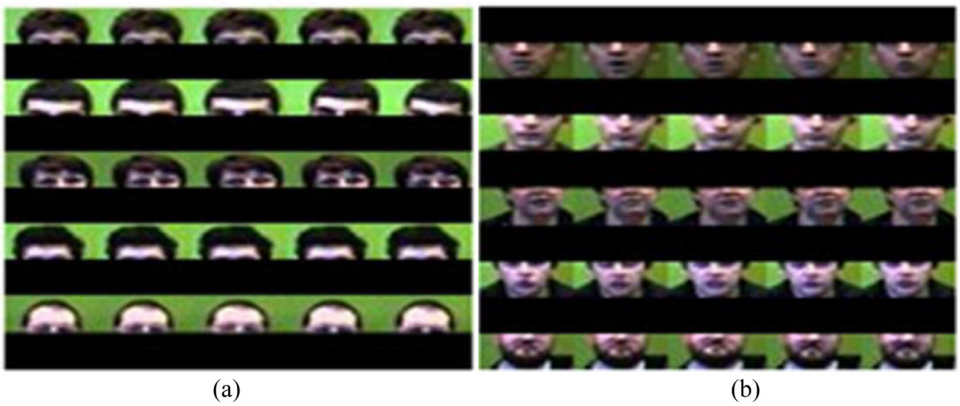


**Fig. 8.** Sample images of (a) the upper half-face and (b) the lower half-face.

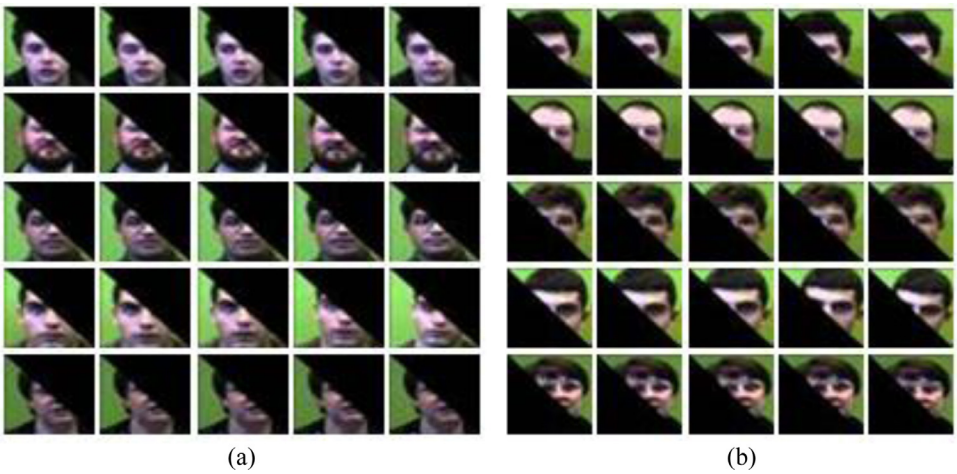


**Fig. 9.** Sample images of (a) the left diagonal half-face and (b) the right diagonal half-face.

performed on F + N2N and F + L2L settings. In these experiments, 1000 images were used for testing in which 10 images of each user are present. The confusion matrix entries and statistical measures are reported in Table 2. It is observed that the accuracy (F + N2N) for nose recognition is superior to (F + L2L) lip recognition. The statistical measures reported in Table 2, error rate, sensitivity, specificity, and precision measures are greater for F + N2N experimental settings compared with F + L2L settings. This suggests that nose features perform better than lip features.

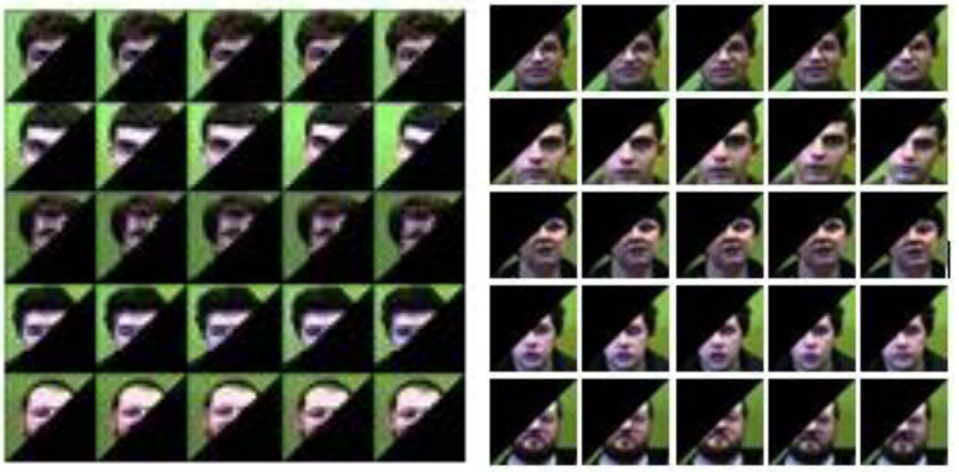


**Fig. 10.** Sample images of (a) the upper diagonal half-face and (b) the lower diagonal half-face.

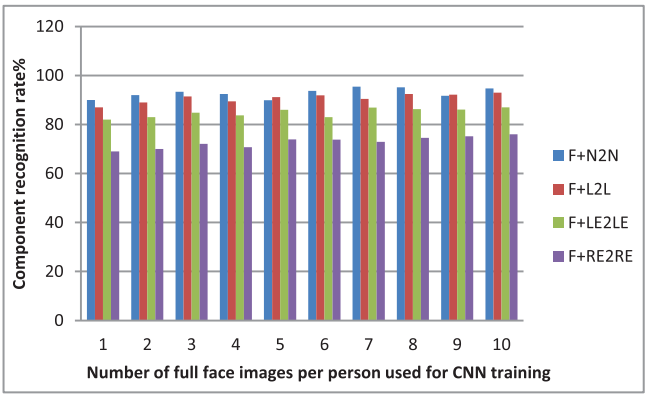


**Fig. 11.** Recognition rates versus the number of the full face images per person used for training the CNN architecture under F + N2N, F + L2L, F + LE2LE, F + RE2RE experimental settings.

**Table 1**
A comparison of handcrafted (HOG and Gabor) feature extraction methods with CNN (recognition rate %).

| HOG | | Gabor | | CNN | |
|---|---|---|---|---|---|
| **Full Face** | **Nose** | **Full Face** | **Nose** | **Full Face** | **Nose** |
| 45 | 42 | 48 | 46 | 98.7 | 95.1 |
| **Full Face** | **Left Ear** | **Full Face** | **Left Ear** | **Full Face** | **Left Ear** |
| 50 | 48 | 48 | 44 | 98.6 | 93.6 |
| **Full Face** | **Right Ear** | **Full Face** | **Right Ear** | **Full Face** | **Right Ear** |
| 52 | 50 | 45 | 43 | 98.7 | 90.2 |
| **Full Face** | **Lip** | **Full Face** | **Lip** | **Full Face** | **Lip** |
| 42 | 40 | 45 | 42 | 98.7 | 74.8 |

ROC is a plot of the true positive rate (TPR) against false positive rate (FPR) and it has been increasingly used for evaluating classifiers to select the most appropriate threshold for a test. The Area under the Curve (AUC) is the probability that a classifier will classify arbitrarily chosen positive samples higher than arbitrarily chosen negative ones. To evaluate a KNN classifier under F + N2F settings and to get different thresholds, K values are varied from 1 to 30. The resultant ROC curve is shown in Fig. 14. The AUC gives the area of 0.95. The closer the value of AUC is to 1, the better the classifier's performance. It depicts that the classifier performs perfectly for F + N2F settings.

The Kappa index has been used as a standard metric for evaluating classifiers since it is statistically robust [8]. To test the stability of the classifier, a KNN classifier is run for different numbers of neighbors by varying the K values from 1 to 30. A box plot is obtained for accuracy and the Kappa index under F + N2F, F + N2N, F + L2L, F + LE2LE and F + RE2RE setting as

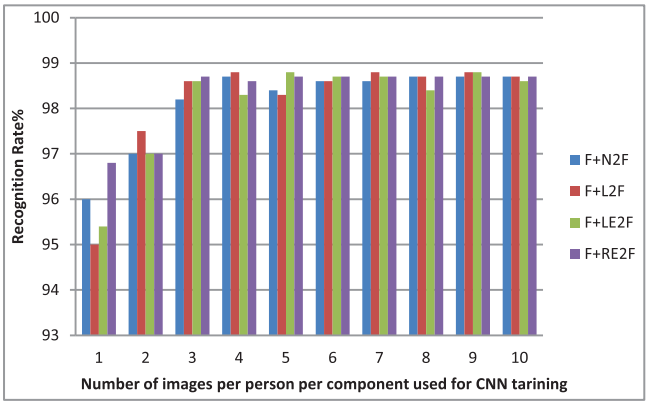


**Fig. 12.** Recognition rates versus number of images used per person per component for training the CNN architecture under F + N2F, F + L2F, F + LE2F, F + RE2F experimental settings.

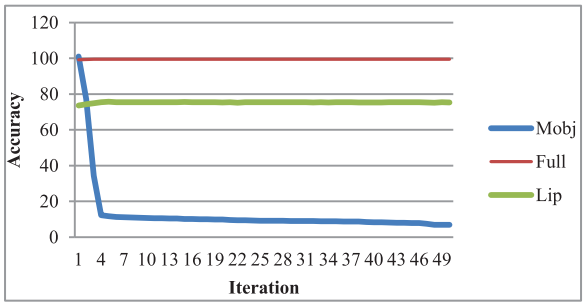


**Fig. 13.** Graph of objective function and face, lip accuracy vs. iteration.

**Table 2**
A range of statistical metrics reported to compare experimental settings F + N2N and F + L2L.

| Statistical metrics | F + N2N | F + L2L |
|---|---|---|
| Accuracy | 0.956 | 0.884 |
| Error | 0.044 | 0.116 |
| Sensitivity | 0.9731 | 0.9179 |
| Specificity | 0.9982 | 0.9952 |
| Precision | 0.956 | 0.884 |

shown in Fig. 15. From the box plot, it is evident that for F + N2F settings, accuracy and Kappa indices are superior to other settings.

### *6.2. Face vs. half-face recognition*

Based on the eight datasets for the half face images, viz. left, right, upper, and lower half, as well as left, right, upper, and lower diagonal, sixteen experimental sets were designed. For experimentation, 1000 images of half faces and 500 images of full faces were utilized for training the CNN and 1000 images of both biometrics were used for testing purposes. By varying the number of full faces used for training, the accuracy of CNN was determined.

(1) F + LH2F: a combination of a full face (F) and the left half face (LH) is applied in the training phase and a full face is used in the testing phase.
(2) F + LH2LH: a combination of a full face (F) and the left half face (LH) is applied in the training phase and the left half face is used in the testing phase.
(3) F + RH2F: a combination of a full face (F) and the right half face (RH) is applied in the training phase and the full face is used in the testing phase.
(4) F + RH2RH: a combination of a full face (F) and the right half face (RH) is applied in the training phase and the right half face is used in the testing phase.

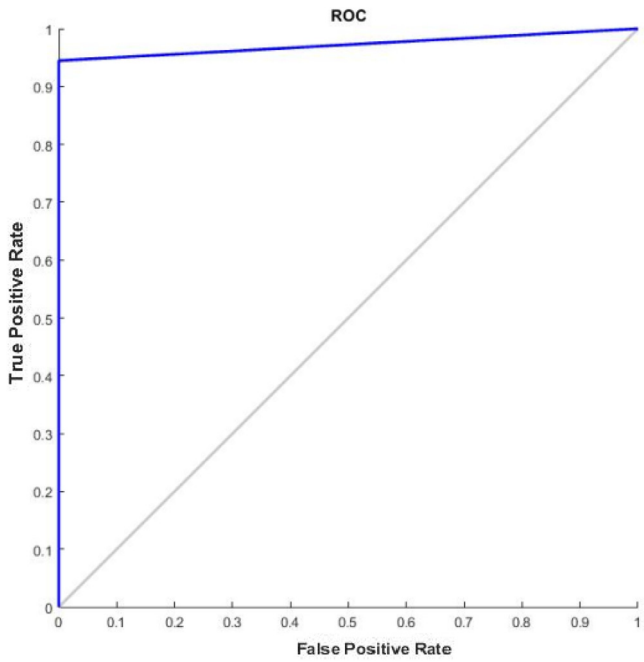


**Fig. 14.** ROC curve for F + N2F experimental settings.

(5) F + UH2F: a combination of a full face (F) and the upper half face (UH) is applied in training phase and full face is used in the testing phase.
(6) F + UH2UH: a combination of a full face (F) and the upper half face (UH) is applied in training phase and upper half face is used in the testing phase.
(7) F + LOH2F: a combination of a full face (F) and the lower half face (LOH) is applied in the training phase and the full face is used in the testing phase.
(8) F + LOH2LOH: a combination of a full face (F) and the lower half face (LOH) is applied in the training phase and the lower half face is used in the testing phase.
(9) F + LD2F: a combination of a full face (F) and the left diagonal face (LD) is applied in the training phase and the full face is used in the testing phase.
(10) F + LD2LD: a combination of a full face (F) and the left diagonal face (LD) is applied in the training phase and left diagonal face is used in the testing phase.
(11) F + RD2F: a combination of a full face (F) and the right diagonal face (RD) is applied in the training phase and the full face is used in the testing phase.
(12) F + RD2RD: a combination of a full face (F) and the right diagonal face (RD) is applied in the training phase and right diagonal face is used in the testing phase.
(13) F + UD2F: a combination of a full face (F) and the upper diagonal face (UD) is applied in the training phase and the full face is used in the testing phase.
(14) F + UD2UD: a combination of a full face (F) and the upper diagonal face (UD) is applied in the training phase and upper diagonal face is used in the testing phase.
(15) F + LOD2F: a combination of a full face (F) and the lower diagonal face (LOD) is applied in the training phase and the full face is used in the testing phase.
(16) F + LOD2LOD: a combination of a full face (F) and the lower diagonal face (LOD) is applied in the training phase and lower diagonal face is used in the testing phase.

Tables 3–10 illustrate the recognition rate for different experimental settings as mentioned previously for a half face. The same trend is observed in all experimental settings as the number of full images used for training decreases, the recognition rate decreases as well. The deep transfer FLDA approach works excellently for any combination of half face images and results in better accuracy.

CNN was experimented with $28 \times 28, 32 \times 32$ and $60 \times 60$ input image sizes and different learning rates of 0.1, 0.01, and 0.001 for 1000 epochs. The best result was obtained for an input size of $32 \times 32$ and a learning rate of 0.001. In Eq. (3), $\lambda$ is the regularization parameter and $\eta$ is the learning rate. The high value of $\lambda$ transfers more information but the very high value of $\lambda$ makes the values of many elements of $M$ zero. On the contrary, the large value of $\eta$ , the distribution difference between the source and target domains was small. However, the very small value of $\eta$ transfers less knowledge. Therefore,

**Table 3**
Recognition accuracy of the left half and full face biometric.

| F + LH | | | |
|---|---|---|---|
| No. of images per person | | Accuracy | |
| LH | F | F + LH2LH | F + LH2F |
| 10 | 5 | 90.7 | 90.4 |
| 10 | 4 | 89.6 | 90.3 |
| 10 | 3 | 88.6 | 85.9 |
| 10 | 2 | 86.7 | 83.4 |
| 10 | 1 | 85.6 | 80.9 |

**Table 4**
Recognition accuracy of right half and full face biometric.

| F + RH | | | |
|---|---|---|---|
| No. of images per person | | Accuracy | |
| RH | F | F + RH2RH | F + RH2F |
| 10 | 5 | 85.6 | 85.7 |
| 10 | 4 | 85.1 | 85.4 |
| 10 | 3 | 84.7 | 83.8 |
| 10 | 2 | 82.7 | 79.8 |
| 10 | 1 | 81.3 | 79.5 |

**Table 5**
Recognition accuracy of the upper half and full face biometric.

| F + UH | | | |
|---|---|---|---|
| No. of images per person | | Accuracy | |
| UH | F | F + UH2UH | F + UH2F |
| 10 | 5 | 80.7 | 86.6 |
| 10 | 4 | 81.7 | 86.5 |
| 10 | 3 | 82.1 | 85.6 |
| 10 | 2 | 80.9 | 85.5 |
| 10 | 1 | 74.6 | 76.1 |

**Table 6**
Recognition accuracy of lower half and full face biometric.

| F + LOH | | | |
|---|---|---|---|
| No. of images per person | | Accuracy | |
| LOH | F | F + LOH2LOH | F + LOH2F |
| 10 | 5 | 85.2 | 84.2 |
| 10 | 4 | 83.6 | 81.9 |
| 10 | 3 | 83.6 | 80.3 |
| 10 | 2 | 81.7 | 79.2 |
| 10 | 1 | 86.1 | 75.1 |

**Table 7**
Recognition accuracy of the diagonally left face and full face.

| F + LD | | | |
|---|---|---|---|
| No. of images per person | | Accuracy | |
| LD | F | F + LD2LD | F + LD2F |
| 10 | 5 | 86.9 | 83.4 |
| 10 | 4 | 86.1 | 82.6 |
| 10 | 3 | 85.7 | 83.5 |
| 10 | 2 | 85.1 | 81.4 |
| 10 | 1 | 87.5 | 79.2 |

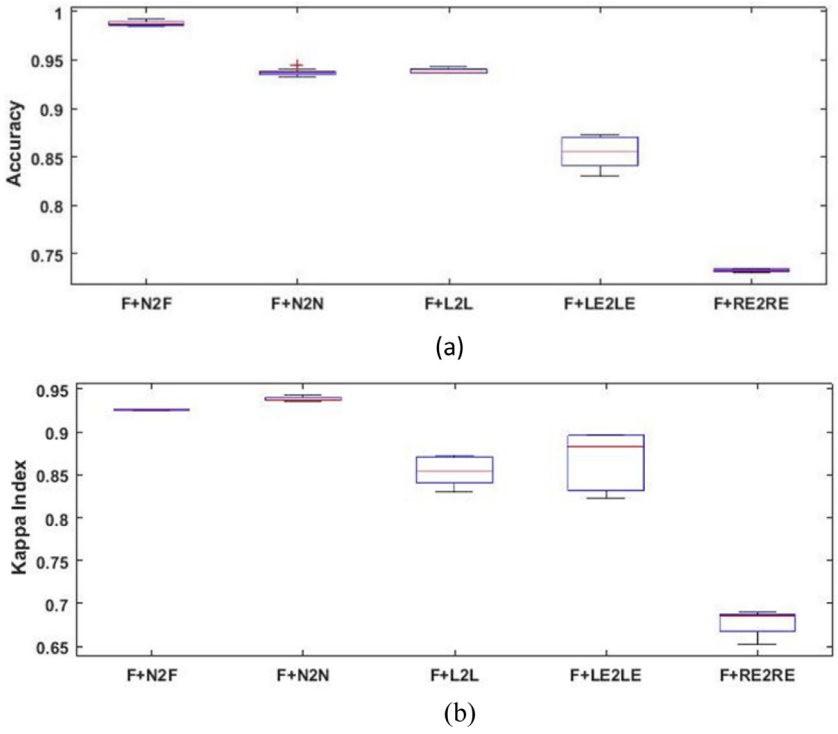


**Fig. 15.** Box plot for (a) average accuracy and (b) average Kappa under F + N2F, F + N2F, F + L2F, F + LE2F, F + RE2F experimental settings.

**Table 8**
Recognition accuracy of the diagonally right face and full face biometric.

| F + RD | | | |
|---|---|---|---|
| No. of images per person | | Accuracy | |
| F + RD | F | F + RD2RD | F + RD2F |
| 10 | 5 | 85 | 88.8 |
| 10 | 4 | 89.8 | 91.6 |
| 10 | 3 | 88.9 | 92.2 |
| 10 | 2 | 88 | 91.7 |
| 10 | 1 | 87.9 | 84.3 |

**Table 9**
Recognition accuracy of the diagonally upper face and full face.

| F + UD | | | |
|---|---|---|---|
| No. of images per person | | Accuracy | |
| UD | F | F + UD2UD | F + UD2F |
| 10 | 5 | 93.5 | 93.8 |
| 10 | 4 | 92.4 | 93.5 |
| 10 | 3 | 92.9 | 93.3 |
| 10 | 2 | 94.4 | 93.3 |
| 10 | 1 | 93.1 | 89.3 |

values of $\eta$ and $\lambda$ are determined by changing one parameter and maintaining the other parameter constant. The best result was obtained for classification accuracy at $\lambda = 100$ and $\eta = 0.1$.

Various research studies have dealt with many applications of transfer learning on support vector machine (SVM) architecture. This study has proposed a generic algorithm for a component-based biometric association based on CNN feature extraction and transfer learning. The application of biometric association is novel and this algorithm can be used for the

**Table 10**
Recognition accuracy of diagonally lower and full face biometric.

| F + LOD | | | |
|---|---|---|---|
| No. of images per person | | Accuracy | |
| LOD | F | F + LOD2LOD | F + LOD2F |
| 10 | 5 | 77.1 | 79.7 |
| 10 | 4 | 72.5 | 81.7 |
| 10 | 3 | 76.1 | 79.4 |
| 10 | 2 | 78 | 83.1 |
| 10 | 1 | 78.8 | 75.7 |

association of other face components. Being a novel approach, there is currently no data available in the relevant literature with which the proposed work can be compared.

## 7. Conclusions

This study has proposed a generic framework for CBFR and association using a CNN architecture under transfer subspace learning for forensic applications. A face and its components are from different domains but they share common information which can be used to transfer obtained knowledge from one domain to another. Three different components of a face, viz., nose, lips, and ears, are chosen for association purposes. These components are unique, stable, and do not change under different facial expressions. The proposed method also works for half-face images. Ears, which form an important component of the face, and the diagonal part of the face, were not considered previously in relevant literature on recognition purposes. In this paper, ears and diagonal parts of the face are considered for association and recognition.

The association between a full face and its components reduces the training time of the system. The system which achieves full face recognition also achieves face component recognition. Therefore, it can be used for holistic face recognition, partial face recognition, as well as component face recognition. Using the standard Faces94 database from the computer vision research project, the study proves that this approach works efficiently for variations in facial expressions. Feature extraction using CNN results in better accuracy against HOG and Gabor features.

Results are compared using different performance matrices: accuracy, Kappa index, confusion matrices, and area under the ROC curve. By comparing different components of the face using the error rate, sensitivity, specificity, and precision measures, it was shown that nose features are better than lip and ear features. A full face works smoothly with any combination of face components and with half-face images as well. The area under the ROC curve for full faces is 0.95 which means that the classifier works well for full faces. To observe the stability of classifiers, a boxplot is plotted for average accuracy and average Kappa index under F + N2F, F + N2F, F + L2F, F + LE2F, F + RE2F experimental settings. It was shown that the accuracy and Kappa index for full faces are better than lip, nose, and ear biometrics. Future work in this area should include the association of a face image and its other components like eyes, mouth, and forehead. Palmprints and fingerprints can also be associated for improving recognition accuracy.

## Funding

This research did not receive any specific grant from funding agencies in the public, commercial, or not-for-profit sectors.

## References

[1] H. Agarwal, M. Agrawal, N. Jain, M. Kumar, Face recognition using principle component analysis, eigenface and neural network, in: Proceedings of the International Conference on Signal Acquisition and Processing, 2010, pp. 310–314.
[2] J. Aggarwal, K. Sato, S. Shah, Partial face recognition using radial basis function networks, in: Proceedings of the IEEE Third International Conference on Automatic Face and Gesture Recognition, 1998, pp. 288–293.
[3] A. Anuse, V. Vyas, A novel training algorithm for convolutional neural network, Complex Intell. Syst. 2 (3) (2016) 221–234.
[4] B. Arbab-Zavar, D.J. Hurley, M.S. Nixon, The ear as a biometric, in: Handbook of Biometrics, Springer, 2008, pp. 131–150.
[5] S. Arunkumar, S. Bhattacharjee, S. Bandyopadhyay, Personal identification from lip-print features using a statistical model, Int. J. Comput. Appl. 55 (13) (2012) 30–34.
[6] M.E. Ashalatha, M.S. Holi, P.R. Mirajkar, Face recognition using local features by LPP approach, in: Proceedings of the International Conference on Circuits, Communication, Control and Computing, Bangalore, 2014, pp. 382–386.
[7] R. Bardia, F. Juefei-Xu, N. Zehngut, Investigating the feasibility of image-based nose biometrics, in: Proceedings of the IEEE International Conference on Image Processing (ICIP), 2015, pp. 522–526.
[8] A. Ben-David, Comparison of classification accuracy using Cohen's Weighted Kappa, Expert Syst. Appl. 34 (2) (2008) 825–832.
[9] M. Bennamoun, A. Mian, R. Owens, An efficient multimodal 2D-3D hybrid approach to automatic face recognition, IEEE Trans. Pattern Anal. Mach. Intell. 29 (11) (2007) 1927–1943.
[10] S. Bentin, N. Sagiv, Structural encoding of human and schematic faces: holistic and part-based processes, J. Cognit. Neurosci. 13 (7) (2001) 937–951.
[11] H.S. Bhatt, N.K. Ratha, R. Singh, M. Vatsa, Improving cross resolution face matching using ensemble-based co-transfer learning, IEEE Trans. Image Process. 23 (12) (2014) 56–69.
[12] K. Bonnen, A.K. Jain, B.F. Klare, Component-based representation in automated face recognition, IEEE Trans. Inf. Forensics Secur. 8 (1) (2013) 239–253.
[13] R. Brunelli, T. Poggio, Face recognition: features versus templates, IEEE Trans. Pattern Anal. Mach. Intell. 15 (10) (1993) 1042–1052.

[14] H. Buelthoff, S. Schumacher, A. Schwaninger, C. Wallraven, Using 3D computer graphics for perception: the role of local and global information in face processing, Appl. Percept. Graph Vis 253 (2007) 19–26.
[15] B. Cao, Y. Chang, W. Gao, S. Shan, W. Zhang, Component-based cascade linear discriminant analysis for face recognition, in: Advances in Biometric Person Authentication, 3338, Commenced Publication in 1973, 2005, pp. 19–79. Lecture Notes in Computer Science.
[16] C.H. Chan, J. Kittler, M. Pietikäinen, M.A. Tahir, Multiscale local phase quantization for robust component-based face recognition using kernel fusion of multiple descriptors, IEEE Trans. Pattern Anal. Mach. Intell. 35 (5) (2013) 1164–1177.
[17] K. Chan, S. Si, D. Tao, Evolutionary cross-domain discriminative hessian eigenmaps, IEEE Trans. Image Process. 19 (4) (2010) 1075–1086.
[18] K. Chan, S. Si, D. Tao, M. Wang, Social image annotation via cross-domain subspace learning, Springer Publ. Multimed. Tools Appl. 56 (2010) 91–108.
[19] W.S. Chen, J. Huang, J. Lai, P. Yuen, Component-based LDA method for face recognition with one training sample, in: Proceedings of the IEEE International Workshop on Analysis and Modeling of Faces and Gestures, 2003, pp. 120–126.
[20] S. Chiller-Glaus, D. Cunningham, A. Schwaninger, C. Wallraven, Processing of identity and emotion in faces: a psychophysical, physiological and computational perspective, Prog. Brain Res. 156 (2006) 321–343.
[21] M. Choras, Ear biometrics based on geometrical feature extraction, Electron. Lett. Comput. Vis. Image Anal. 5 (3) (2005) 84–95.
[22] M. Choras, The lip as a biometric, Pattern Anal. Appl. 13 (1) (2010) 105–112.
[23] B.H. Chou, H. Shao, E. Suzuki, B. Tong, Linear semisupervised projection clustering by transferred centroid regularization, J Intell Inf Syst 39 (2012) 461–490.
[24] G. Cong, V. Gopalkrishnan, K. Sim, A. Zimek, A survey on enhanced subspace clustering, Data Min. Knowl. Disc. 26 (2) (2013) 332–397.
[25] G. Davies, H. Ellis, J. Shepherd, Studies of cue saliency, in: Perceiving and Remembering Faces, 1, Academic Press Series in Cognition and Perception, 1981, pp. 105–131.
[26] M. De Bruijne, M.A. Ikram, A. Van Opbroek, M.W. Vernooij, Transfer learning improves supervised image segmentation across imaging protocols, IEEE Trans. Med. Imaging 34 (5) (2015) 1018–1030.
[27] M.A. Elenien, M. Sharkas, Eigenfaces vs. fisherfaces vs. ICA for face recognition; a comparative study, in: Proceedings of the International Conference on Signal Processing, 2008, pp. 914–919.
[28] J.M. Fellous, N. Kreuger, C.V. Malsburg, L. Wiskott, Face recognition by elastic bunch graph matching, IEEE Trans. Pattern Anal. Mach. Intell. 19 (7) (1997) 775–779.
[29] S. Feng, Y. Guo, Y. Lei, X. Zhou, An efficient 3D partial face recognition approach with single sample, in: Proceedings of the IEEE 11th Conference on Industrial Electronics and Applications, 2016, pp. 994–999.
[30] Y Fu, J. Luo, M. Shao, S. Xia, Understanding kin relationship in a photo, IEEE Trans. Multimed. 14 (4) (2012) 1046–1056.
[31] X. Gao, J. Li, D. Liu, C. Peng, N. Wang, Composite face sketch recognition based on components, in: Proceedings of the International Conference on Wireless Communications & Signal Processing, 2016, pp. 1–5.
[32] B. Geng, S. Si, D. Tao, Bregman divergence-based regularization for transfer subspace learning, IEEE Trans. Knowl. Data Eng. 22 (7) (2010) 929–942.
[33] J. Gold, P. Mundy, B. Tjan, The perception of a face is no more than the sum of its parts, Psychol. Sci. 23 (4) (2012) 427–434.
[34] A. Gumede, M. Gwetu, S. Viriri, Hybrid component-based face recognition, in: Proceedings of the Conference on Information Communication Technology and Society, 2017, pp. 1–6.
[35] S. Gutta, V. Philomin, M. Trajkovic, An investigation into the use of partial-faces for face recognition, in: Proceedings of the International Conference on Automatic Face and Gesture Recognition, 2002, pp. 33–38.
[36] L. He, Z. He, H. Li, Z. Sun, Q. Zhang, Multiscale representation for partial face recognition under near infrared illumination, in: Proceedings of the IEEE 8th International Conference on Biometrics Theory, Applications and Systems, 2016, pp. 1–7.
[37] C. Hou, M. Lin, Y. Wu, S. Yang, C. Zhang, A general framework for transfer sparse subspace learning, Neural. Comput. Appl. 21 (2012) 1801–1817.
[38] J. Hu, J. Lu, Y. Tan, Robust partial face recognition using instance-to-class distance, 2013 Visual Communications and Image Processing (VCIP), Kuching, 2013, pp. 1–6, doi:10.1109/VCIP.2013.6706353.
[39] A.K. Jain, B. Klare, U. Park, Face recognition: some challenges in forensics, in: Proceedings of the 9th IEEE International Conference on Automatic Face and Gesture Recognition (FG), 2011, pp. 726–733.
[40] I. Jarudi, J. Sadr, P. Sinha, The role of eyebrows in face recognition, Perception 32 (2006) 285–293.
[41] R.R. Jillela, U. Park, A. Ross, Periocular biometrics in the visible spectrum, IEEE Trans. Inf. Forensics Secur. 6 (1) (2011) 96–106.
[42] R.S. Kute, V. Vyas, Biometric association using transfer subspace learning, in: Proceedings of the IEEE Region 10 Conference (TENCON), 2016, pp. 1384–1387.
[43] F. Li, M. Tistarelli, H. Wechsler, Robust fusion using boosting and transduction for component-based face recognition, in: Proceedings of the International Conference on Control, Automation, Robotics, and Vision, 2008, pp. 434–439.
[44] SZ Li, S. Liao, A.K. Jain, Partial face recognition: Alignment-free approach, in: Proceedings of the IEEE Transactions on Pattern Analysis and Machine Intelligence, 35, 2013, pp. 1193–1205.
[45] J. Lu, Y.P. Tan, R. Weng, Robust point set matching for partial face recognition, IEEE Trans. Image Process. 25 (3) (2016) 1163–1176.
[46] A.M. Martinez, Recognizing imprecisely localized, partially occluded, and expression variant faces from a single sample per class, IEEE Trans. Pattern Anal. Mach. Intell. 24 (6) (2002) 748–763.
[47] New Identity Authentication Method: Nose biometrics Drupal, www.homelandsecuritynewswire.com/new-identity-authentication-method-nose-biometrics.
[48] J. Pan, Q. Yang, A Survey on transfer learning, IEEE Trans. Knowl. Data Eng. 22 (10) (2010) 1345–1359.
[49] S. Gutta, H. Wechsler, Partial Faces for Face Recognition: Left vs Right Half, in: N. Petkov, M.A. Westenberg (Eds.), Computer Analysis of Images and Patterns. CAIP 2003, vol. 2756, Springer, Berlin, Heidelberg, 2003 Lecture Notes in Computer Science.
[50] E. Walia, Face recognition using improved fast PCA algorithm, Cong. Image Signal Process. (2008) 554–558.